

## Ray-wave correspondence in chaotic dielectric billiards

Takahisa Harayama<sup>1</sup> and Susumu Shinohara<sup>2</sup>

<sup>1</sup>*Department of Applied Physics, School of Advanced Science and Engineering, Waseda University, 3-4-1 Okubo, Shinjuku-ku, Tokyo 169-8555, Japan*

<sup>2</sup>*NTT Communication Science Laboratories, NTT Corporation, 2-4 Hikaridai, Seika-cho, Soraku-gun, Kyoto 619-0237, Japan*

(Received 15 June 2015; published 19 October 2015)

Based on the reformulation of the boundary integral equations recently derived by Creagh, Hamdin, and Tanner [*J. Phys. A: Math. Theor.* **46**, 435203 (2013)] together with semiclassical (short wavelength) approximation, we theoretically show that low-loss resonances of a fully chaotic dielectric billiard can be related with ray dynamical orbits whose intensities are weighted by the Fresnel reflection and transmission coefficients. In addition, it is revealed that intensity localization spots observed in the phase-space representation of an individual resonance wave function are ray-dynamically correlated.

DOI: [10.1103/PhysRevE.92.042916](https://doi.org/10.1103/PhysRevE.92.042916)

PACS number(s): 05.45.Mt, 42.55.Sa, 05.10.-a, 42.65.Sf

Ray and wave dynamics in microcavities are analogous to the classical and quantum descriptions of particle dynamics in billiards, which have extensively been studied as typical models for ergodic and quantum-chaos theories in mathematics and physics [1–11]. Microcavity lasers whose billiard dynamics is chaotic (chaotic billiard lasers, in short [12]) have attracted much attention not only because they are interesting from a fundamental-physics viewpoint but also because they enable novel applications that cannot be implemented by conventional lasers [12–24].

Chaotic billiard lasers are able to emit lights in all two-dimensional directions. One of their important characteristics is a far-field pattern of the light intensity, which has been experimentally measured for various microcavity shapes [14,17,20–22,25–28]. The far-field pattern can be numerically calculated by the wave and ray models. The wave model is based on resonance wave functions that are the solutions of the Helmholtz equation under relevant boundary conditions [20–22,29,30]. On the other hand, the ray model is constructed in a somewhat ad hoc manner, by describing the dielectric boundary by the Fresnel coefficients. Although the ray model has not been fully validated, it has been frequently employed and shown to be capable of very well reproducing experimentally measured far-field patterns as well as numerical results calculated by the wave model [13,14,17–22,27,31–38]. Also, the importance of the ray dynamics weighted by the Fresnel coefficients has been demonstrated in the application of the fractal Weyl law to the resonances of dielectric billiards [39]. However, less theoretical studies have been performed to explain the remarkable ray-wave correspondences in chaotic dielectric billiards.

The purpose of this paper is to provide a theoretical explanation on the reason why the ray model can reproduce the results of the wave model so well. By semiclassical (short wavelength) theory based on the recently established formulation of the boundary integral equation by Creagh, Hamdin, and Tanner [40], we show that low-loss resonances correspond to the steady intensity distribution of the ray model. The key idea here is the iterative application of the transfer operator derived by Creagh, Hamdin, and Tanner to a wave function. It is assumed in this paper that the dielectric billiard has a convex shape and its ray dynamics is fully chaotic.

First, we briefly review the wave model [20–22,29,30]. The light fields are considered as the classical electromagnetic fields, and the resonant modes of a dielectric billiard are obtained as the eigenstates of the Helmholtz equation derived from the Maxwell equations,

$$(\nabla^2 + n^2 k^2)\psi = 0, \quad (1)$$

where  $k$  is a wave number and  $n$  is a refractive index which changes sharply at the billiard edge. Equation (1) describes the light confinement by the dielectric billiard, where the refractive index inside the billiard  $n_{\text{in}}$  is higher than that outside the billiard  $n_{\text{out}}$ . Equation (1) is solved with the outgoing radiation condition at infinity. Since this condition imposes a constant emission without a gain, the resulting eigenstates are decaying. The decaying eigenstates are called resonances. A resonance is characterized by a complex wave number, whose real part represents the frequency, while the imaginary part the decay rate.

Next, we explain the ray model [13,16,31,34–38]. For a dielectric billiard, some portion of the intensity escapes from the billiard, whenever a ray orbit hits the boundary, obeying the Fresnel reflection and transmission coefficients  $\mathcal{R}$  and  $\mathcal{T}$ , where  $\mathcal{T} = 1 - \mathcal{R}$ .  $\mathcal{R}$  can be expressed as a function of incident and transmission angles  $\varphi$  and  $\varphi_t$  subject to Snell's law  $n_{\text{in}} \sin \varphi = n_{\text{out}} \sin \varphi_t$ . For example, for TM polarization, we have  $\mathcal{R} = [\sin(\varphi - \varphi_t) / \sin(\varphi + \varphi_t)]^2$ . When a ray orbit is totally internally reflected (i.e.,  $|\sin \varphi| > n_{\text{out}}/n_{\text{in}}$ ), we have  $\mathcal{R} = 1$  (i.e.,  $\mathcal{T} = 0$ ) [41]. In the ray model, it is supposed that a reflected ray, which had the intensity  $\epsilon$  before the reflection has the intensity  $\mathcal{R}\epsilon$ , while the transmitted ray has the intensity  $\mathcal{T}\epsilon$ . Tracing ray dynamics for an ensemble of rays and collecting transmitted intensities as a function of the polar angle  $\varphi$ , one obtains a far-field emission pattern for the ray model.

Recently, Creagh, Hamdin, and Tanner succeeded in reformulating the boundary integral equations. This reformulation brings a clearer viewpoint in understanding wave phenomena in a region surrounded by boundaries [40]. Here we briefly review this new formalism as we apply it to bridge the gap between the ray and wave models for fully chaotic dielectric billiards.

Equation (1) combined with the outgoing radiation condition can be rewritten by the conventional boundary integral

equation as

$$\psi = \hat{G}_0 \mu - \hat{G}_1 \psi, \quad (2)$$

where  $\mu$  is a normal derivative of the wave function,

$$\mu(s) \equiv \frac{\partial \psi(s)}{\partial v_s}, \quad (3)$$

and the Green operators  $\hat{G}_0$  and  $\hat{G}_1$  are defined as

$$\hat{G}_0(s)\mu(s) \equiv \lim_{\mathbf{r} \rightarrow s} \oint_{\partial B} ds' G_0(\mathbf{r}, s'; nk) \mu(s'), \quad (4)$$

and

$$\hat{G}_1 \psi(s) \equiv \lim_{\mathbf{r} \rightarrow s} \oint_{\partial B} ds' \frac{\partial G_0(\mathbf{r}, s'; nk)}{\partial v_{s'}} \psi(s'). \quad (5)$$

In the above,  $\psi(s)$  denotes the solution of Eq. (1) restricted on the billiard boundary where  $s$  denotes an arc-length coordinate, and the free Green function is defined by

$$(\nabla^2 + n^2 k^2) G_0(\mathbf{r}, \mathbf{r}'; nk) = -\delta(\mathbf{r} - \mathbf{r}'). \quad (6)$$

Creagh, Hamdin, and Tanner [40] decomposed the Green operators into a singular and a regular part as  $\hat{G}_0 = \hat{G}_0^{\text{sing}} + \hat{G}_0^{\text{reg}}$  and  $\hat{G}_1 = \hat{G}_1^{\text{sing}} + \hat{G}_1^{\text{reg}}$ , and rewrote Eq. (2) using an outgoing wave  $\psi_+(s)$  from the billiard boundary and  $\psi_-(s)$  an incoming wave, where  $\psi_+ = \hat{G}_0^{\text{sing}} \mu - \hat{G}_1^{\text{sing}} \psi$  and  $\psi_- = \hat{G}_0^{\text{reg}} \mu - \hat{G}_1^{\text{reg}} \psi$ , and the resonance wave function  $\psi$  of the solution for the Helmholtz Eq. (1) is given by  $\psi(s) = \psi_+(s) + \psi_-(s)$ . Then  $\psi_+(s)$  satisfies the following equation expressed as the transfer operator form,

$$\psi_+ = \hat{T} \psi_+, \quad (7)$$

where  $\hat{T} \equiv \hat{r} \hat{S}$  and  $\psi_-(s) = \hat{S} \psi_+(s)$ , and  $\hat{r}$  corresponds to the reflection while  $\hat{S}$  the propagation.

The resonances can be obtained as the complex wave numbers satisfying the secular equation,

$$\det[\hat{I} - \hat{T}(k)] = 0. \quad (8)$$

This type of equation can be derived for the Dirichlet or Neumann boundary conditions without the reformulation of the conventional boundary integral Eq. (2). However, for dielectric billiards, the boundary integral equations include both wave functions and their normal derivatives, and the secular equation like Eq. (8) had not been derived, although the semiclassical transfer operator method has been proposed [42]. This newly derived reformulation of the boundary integral equation plays an essential role in understanding how the ray model arises from the wave description.

Creagh, Hamdin, and Tanner [40] obtained the following short wavelength approximations. The ray-dynamical limit  $r(s, s')$  of  $\hat{r}$  is the Fresnel reflection coefficients;  $\tan[\varphi(s, s') - \varphi_t(s, s')]/\tan[\varphi(s, s') + \varphi_t(s, s')]$  for TE modes and  $-\sin[\varphi(s, s') - \varphi_t(s, s')]/\sin[\varphi(s, s') + \varphi_t(s, s')]$  for TM modes, where  $\varphi(s, s')$  denotes the angle between the vector  $[\mathbf{r}(s') - \mathbf{r}(s)]$  and the outer normal vector  $\mathbf{n}(s')$  at the point  $s'$ , and  $\varphi_t(s, s')$  denotes the transmission angle depending on the refractive indices as well as the incident angle.

The semiclassical limit of the kernel of  $\hat{S}$  is given by

$$S(s, s') \simeq \sqrt{\frac{nk}{2\pi i} \frac{1}{\cos \varphi(s, s')} \frac{\partial^2 L}{\partial s \partial s'}} \cos \varphi(s', s) e^{inkL}, \quad (9)$$

where  $L = L(s, s')$  denotes the distance between the points  $s$  and  $s'$ , i.e.,  $L(s, s') \equiv |\mathbf{r}(s) - \mathbf{r}(s')|$ . These semiclassical approximations provide a connection between wave phenomena and ray orbits. For example, the straightforward semiclassical limit of the left-hand side of Eq. (8) yields the Gutzwiller-Voros  $\zeta$  function [42–45] for dielectric billiards. The resulting formula includes the refractive indices in the weights of the conventional periodic orbit contributions [46,47].

In the field of optics, an iterative method developed by Fox and Li has been widely used for calculating resonant modes for optical cavities [48–51]. The Fox-Li method is based on the same boundary integral equation as Eq. (2), but is very different from a straightforward method such as the boundary element method [30]. It is usually applied to conventional one-dimensional cavities consisting of two perfect end mirrors. The method computes beam propagation from one end mirror to the other, and the round-trip calculations are repeated with an initial light-field distribution. Although reflection losses at the end mirrors are not considered, the light intensities are always decreasing under iterative beam propagation, where the losses are caused by the leakage through long nonreflecting side-wall mirrors. As the result of the iterative beam propagation, the light-field distribution finally converges to that of a resonant mode.

The Fox-Li method cannot be directly applied to two-dimensional dielectric billiards, because their boundaries cannot be simply divided into perfect mirrors and leaky mirrors as in the conventional one-dimensional cavities. However, the transfer operator of Creagh, Hamdin, and Tanner [40] allows us to formulate a leaky wave propagation similar to the Fox-Li method even for two-dimensional dielectric billiards. To illustrate this idea, we consider the following mapping of the wave function by the transfer operator with a real wave number in the semiclassical limit,

$$\psi_{+,1}(s) = \oint_{\partial B} ds' r(s, s') S(s, s') \psi_{+,0}(s'), \quad (10)$$

where the initial outgoing wave function  $\psi_{+,0}$  on the billiard boundary is propagated, reflected, and transmitted to construct the outgoing wave function  $\psi_{+,1}$ . Because transmission occurs at the billiard boundary and the kernel is calculated with a real wave number, the intensity of  $\psi_{+,1}$  is smaller than that of  $\psi_{+,0}$ . Thus, when the outgoing wave function is mapped iteratively  $m$  times by the transfer operator and  $m$  is large enough, the wave function  $\psi_{+,m}$  converges to the most slowly decaying eigenmode  $\phi_+(s)$  contained in  $\psi_{+,0}(s)$ , where  $\phi_+(s)$  is characterized by the decay rate  $\gamma \bar{L}$  with  $\bar{L}$  being the average of the increase of the length of ray orbits at one mapping on the billiard boundary, i.e.,  $\psi_{+,m}(s) \simeq e^{-\gamma \bar{L} m} \phi_+(s)$  when  $m \gg 1$ . Depending on the choice of the initial wave function  $\psi_{+,0}$ , the most slowly decaying eigenmode  $\phi_+$  can change. This situation corresponds to the existence of infinitely many invariant measures in open systems.

The iterative mapping is written explicitly as follows,

$$\begin{aligned} \psi_{+,m}(s) = & \oint_{\partial B} \cdots \oint_{\partial B} ds_0 \cdots ds_{m-1} r(s, s_{m-1}) S(s, s_{m-1}) \cdots r(s_1, s_0) S(s_1, s_0) \psi_{+,0}(s_0) = \oint_{\partial B} \cdots \oint_{\partial B} ds_0 \cdots ds_{m-1} \left( \frac{nk}{2\pi i} \right)^{m/2} \\ & \times \left[ \prod_{j=0}^{m-1} \frac{\cos \varphi(s_{j+1}, s_j)}{\cos \varphi(s_j, s_{j+1})} \frac{\partial^2 L}{\partial s_j \partial s_{j+1}} \right]^{1/2} \left[ \prod_{j=0}^{m-1} r(s_j, s_{j+1}) \right] \exp \{ inkL(s, s_{m-1}, \dots, s_0) \} \psi_{+,0}(s_0), \end{aligned} \quad (11)$$

where  $s_m \equiv s$  and the sum of  $L(s_j, s_{j+1})$  defines the total length  $L(s, s_{m-1}, \dots, s_0) \equiv \sum_{i=0}^{m-1} L(s_i, s_{i+1})$ . We apply the stationary phase approximation to the multiple integrals except for the integral concerning  $s_0$ , and obtain

$$\begin{aligned} \psi_{+,m}(s) \simeq & \oint_{\partial B} ds_0 \sum_{\text{r.o.}} \frac{\sqrt{\frac{nk}{2\pi i}}}{\sqrt{\cos \varphi(s_{m-1}^*, s)}} \left( \prod_{j=0}^{m-1} r(s_j^*, s_{j+1}^*) \right) \left| \left( \prod_{j=0}^{m-1} M_{j+1 \leftarrow j} \right) \right|_{12}^{-1/2} \\ & \times \exp \left\{ inkL(s, s_{m-1}^*, \dots, s_1^*, s_0) - \frac{\sigma}{2} \pi i \right\} \sqrt{\cos \varphi(s_1^*, s_0)} \psi_{+,0}(s_0). \end{aligned} \quad (12)$$

Here the summation should be taken over all of the ray orbits subject to the law of reflection, which start from  $s_0$  and reach  $s$  in  $m-1$  reflections at the points  $s_1^*, \dots, s_{m-1}^*$ , and  $\sigma$  is the number of focal points of the ray orbit.  $M_{j+1 \leftarrow j}$  represents the matrix linearized in the vicinity of the ray orbit in the Birkhoff coordinates, i.e.,

$$\begin{pmatrix} \delta s_{j+1} \\ \delta(\sin \varphi_{j+1}) \end{pmatrix} = M_{j+1 \leftarrow j} \begin{pmatrix} \delta s_j \\ \delta(\sin \varphi_j) \end{pmatrix}, \quad (13)$$

and it is calculated by the geometrical information of the ray orbit as

$$M_{j+1 \leftarrow j} = - \begin{pmatrix} 1 & 0 \\ 0 & \cos \varphi_{j+1} \end{pmatrix} \begin{pmatrix} \frac{1}{\cos \varphi_{j+1}} & 0 \\ \frac{K(s_{j+1})}{\cos \varphi_{j+1}} & 1 \end{pmatrix} \begin{pmatrix} 1 & L(s_j, s_{j+1}) \\ 0 & 1 \end{pmatrix} \begin{pmatrix} \cos \varphi_j & 0 \\ K(s_j) & 1 \end{pmatrix} \begin{pmatrix} 1 & 0 \\ 0 & \frac{1}{\cos \varphi_j} \end{pmatrix}, \quad (14)$$

where  $\varphi_j \equiv \varphi(s_{j+1}, s_j)$ , and  $K(s_j)$  is the curvature of the billiard boundary measured by the outer normal at the point  $s_j$ .

The ray orbits connecting the points  $s_0$  and  $s$  proliferate exponentially with the exponent of topological entropy when  $m$  is large enough. On the other hand, the denominator of the ray orbit contribution in the ray orbit sum expressed by the product of the linearized matrices increases exponentially with the exponent of a half of the Lyapunov exponent. Thus, the situation looks similar to that of the periodic orbit sum of the Gutzwiller formula [44]. However, the product of the Fresnel coefficients of the ray orbit contribution decreases exponentially, so that the number of dominantly contributing ray orbits inside the billiard decreases exponentially with the exponent similar to the escape rate. Accordingly, as far as the difference of the refractive indices inside and outside the billiard is small, the ray orbit sum can be expected to be absolutely convergent. Otherwise, it might be conditionally convergent at best.

Equation (12) connects the ray model with the wave function. Before discussing the implications of Eq. (12), let us review the steady distribution of the ray model. In the course of ray dynamical time evolution, the intensities of ray orbits decrease due to the transmission described by Fresnel's law. For example, a ray orbit of the bouncing-ball mode type loses its intensity very rapidly, while a ray orbit confined by total internal reflection never decays. For a fully chaotic billiard, because any ray orbit (except for those with zero measure) will violate the critical angle condition at some points, the intensities of almost all orbits are decreasing. It has been numerically shown that the total intensity of a ray

ensemble initially distributed uniformly over the phase space is exponentially decaying asymptotically [21,34]. Factoring out this exponential decay, one can obtain a steady intensity distribution in the phase space. In Fig. 1(b), we show the steady intensity distribution obtained by the ray model for Bunimovich's stadium dielectric billiard [defined in Fig. 1(a)] with  $n_{\text{in}} = 3.3$  and  $n_{\text{out}} = 1$  (for a numerical procedure to generate this distribution, see Ref. [34]), where the darker the color, the stronger the intensity. Here, the phase space is spanned by the Birkhoff coordinates  $(s, \sin \varphi)$ , where  $s$  and  $\varphi$  are the arc-length along the billiard boundary and the incident angle, as defined in Fig. 1(a). The structure of the steady phase-space intensity distribution is closely related with that of the unstable manifolds from the unstable periodic points located close to the critical angle for total internal reflection (i.e.,  $\sin \varphi = \pm n_{\text{in}}/n_{\text{out}}$ ) [38]. We note that the white (i.e., very leaky) regions around  $(s, \sin \varphi) = (0.25, 0)$  and  $(s, \sin \varphi) = (0.75, 0)$  correspond to the phase-space areas around the bouncing-ball orbits (i.e., normal-incidence orbits bouncing between the two linear segments of the stadium billiard).

Equation (12) can be viewed as the wave-model counterpart of the intensity mapping of the ray model. Because of the multiplicative effect of the Fresnel reflection coefficient in Eq. (12) similar to that of the ray model, we can suppose that the most slowly decaying mode of Eq. (12) (in the sense of a Fox-Li type iteration) would have a phase-space intensity distribution whose support is contained in the support of the steady phase-space intensity distribution of the ray model. On

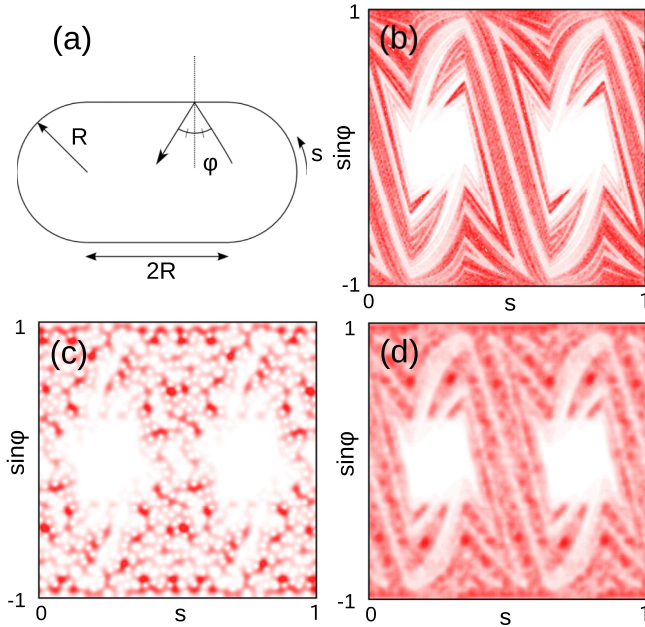


FIG. 1. (Color) (a) Geometry of the stadium billiard and the definition of the variables  $s$  and  $\varphi$  for the Birkhoff coordinates  $(s, \sin \varphi)$ . (b) Phase-space intensity distribution obtained by the ray mode for the stadium dielectric billiard with refractive index  $n_{\text{in}} = 3.3$  (refractive index outside the billiard is  $n_{\text{out}} = 1$ ). (c) Husimi distribution of the wave function for a low-loss mode with the wave number  $k = 99.98 - i 0.0058$ . The wave function is calculated by numerically solving Eq. (1) for the stadium dielectric billiard imposing the boundary condition for TM polarization. (d) The average of the Husimi distributions for 28 low-loss modes in the wave number region  $\text{Re } k \in [99.95, 100.05]$  and  $\text{Im } k > -0.0088$ . In (b)–(d), the darker the color, the stronger the intensity, and the horizontal axis  $s$  is normalized by the total boundary length.

the other hand, a fast-decaying mode would have a phase-space intensity distribution whose support does not overlap so much with that of the steady phase-space intensity distribution of the ray model. Here we only focus our attention on the intensity of the wave function, but a detailed analysis of phase information in Eq. (12) might be useful for studying the effects such as Goos-Hänchen shift as has been done for a circular dielectric billiard in Ref. [40].

Mathematically, there is a gap between the resonances of the stationary problem of Eq. (1) and the decaying modes of the iterative formalism applied to Eq. (1). However, physically it seems natural to relate low-loss modes of the former to slowly decaying modes of the latter. Assuming this relation, we examine if the ray-wave correspondence discussed above based on Eq. (12) can be applied to the interpretation of the wave functions of low-loss resonances. For this purpose, we employ here the Husimi phase-space distribution of a wave function corresponding to an incoming ray to the billiard boundary [52]. In Figs. 1(c) and 1(d), we respectively show the Husimi distribution for a single low-loss resonance for the stadium dielectric billiard with the wave number  $k = 99.98 - i 0.0058$  and the distribution obtained by averaging the Husimi distributions for 28 low-loss modes detected in the wave number region  $\text{Re } k \in [99.95, 100.05]$

and  $\text{Im } k > -0.0088$ . The resonances and wave functions are numerically calculated by the boundary element method [30], imposing the boundary condition for TM polarization and the outgoing radiation condition at the infinity. The comparison between Figs. 1(b) and 1(c) reveals that high-intensity phase-space spots for the Husimi distribution are supported on the ray-dynamical steady phase-space intensity distribution, which coincides with the prediction of Eq. (12) that a low-loss mode has an intensity distribution whose support is contained in that of the ray-dynamical steady intensity distribution.

Moreover, comparing Figs. 1(b) and 1(d), we can find that the average of Husimi distributions for many low-loss modes closely reproduces the ray-dynamical intensity distribution. This finding suggests that taking a uniform phase-space distribution as the initial condition for the ray model is physically meaningful in the sense that it generates a ray-dynamical distribution corresponding to low-loss resonances. We note that such a collective correspondence explains the reason why the ray model reproduces experimental data better for multimode lasing than for a single-mode lasing [36,37,53,54].

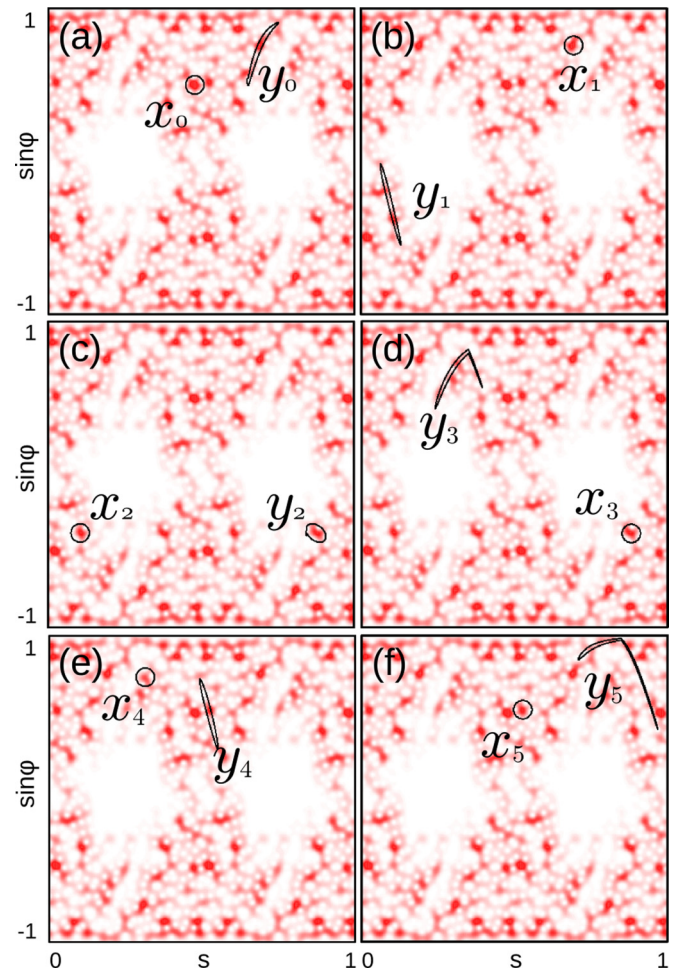


FIG. 2. (Color) Husimi distribution for a low-loss mode with the wave number  $k = 99.98 - i 0.0058$  [same as Fig. 1(c)], superposed with information on how a circular area labeled by  $x_j$  ( $j = 0, \dots, 5$ ) containing a high-intensity spot is mapped to another (elongated) area labeled by  $y_j$  ( $j = 0, \dots, 5$ ) under the ray dynamics.

We also note that the ray-wave correspondence shown here looks similar to classical-quantum correspondence observed in open quantized chaotic maps [55–59].

In addition, even for a single-wave function, Eq. (12) suggests the existence of a correlation between the wave function values at two different boundary points,  $\varphi_{+,j}(s')$  and  $\varphi_{+,j}(s)$ , through ray orbits connecting  $s'$  and  $s$ . In general, there are multiple ray orbits reaching the point  $s'$  with different incident angles and momenta. These different momentum contributions can be resolved by the phase-space representation of the wave function. In order to check if we can observe a ray-dynamical correlation for the boundary values of a single resonance wave function, we numerically investigated how the area corresponding to a high-intensity spot of the Husimi distribution is mapped by the ray dynamics. In Figs. 2(a)–2(f), the Husimi distribution of the wave function for the low-loss mode with the wave number  $k = 99.98 - i0.0058$  is superposed with the information on how a circular area located around a high-intensity spot of the Husimi distribution is mapped by the ray dynamics. The circular areas are denoted by black circles and labeled by  $x_j (j = 0, \dots, 5)$ , while the mapped (elongated) areas are labeled by  $y_j (j = 0, \dots, 5)$ . In Fig. 2, we can see that the mapped area  $y_j (j = 0, \dots, 4)$  significantly

overlaps with the other high-intensity spot(s) of the Husimi distribution, although for  $y_5$ , the mapped area is so elongated that the overlap with a high-intensity spot is subtle. We show here the ray-dynamical correlation only for a specific low-loss mode, but we confirmed that this property can be generally observed for the resonances of the stadium dielectric billiard. We expect that the semiclassical formulation of the Husimi distribution would enable more detailed understanding on the observed ray-dynamical correlation. We note that similar ray-dynamical correlations in the phase-space representation of an eigenfunction have been observed for a closed quantized chaotic map [60].

In summary, for fully chaotic dielectric billiards with convex shape, we obtained the semiclassical approximation for the iteration of the transfer operator recently derived by Creagh, Hamdin, and Tanner [40], which connects the intensity distributions of the ray and wave models. Through this semiclassical approximation, we presented a theoretical explanation on the correspondence between the phase-space pattern of a low-loss resonance wave function and the steady phase-space distribution of the ray model.

The authors thank Prof. Jan Wiersig for useful discussions.

- 
- [1] Y. G. Sinai, *Russ. Math. Surv.* **25**, 137 (1970).  
 [2] L. A. Bunimovich, *Commun. Math. Phys.* **65**, 295 (1979).  
 [3] S. W. McDonald and A. N. Kaufman, *Phys. Rev. Lett.* **42**, 1189 (1979).  
 [4] O. Bohigas, M. J. Giannoni, and C. Schmit, *Phys. Rev. Lett.* **52**, 1 (1984).  
 [5] E. J. Heller, *Phys. Rev. Lett.* **53**, 1515 (1984).  
 [6] S. Zelditch and M. Zworski, *Commun. Math. Phys.* **175**, 673 (1996).  
 [7] P. Gaspard, *Chaos, Scattering and Statistical Mechanics*, (Cambridge University Press, Cambridge, UK, 1998).  
 [8] H.-J. Stöckmann, *Quantum Chaos: An Introduction* (Cambridge University Press, Cambridge, England, 1999).  
 [9] K. Nakamura and T. Harayama, *Quantum Chaos and Quantum Dots* (Oxford University Press, Oxford, 2004).  
 [10] A. D. Stone, *Phys. Today* **58**, 37 (2005).  
 [11] E. G. Altmann, J. S. E. Portela, and T. Tél, *Rev. Mod. Phys.* **85**, 869 (2013).  
 [12] A. D. Stone, *Nature* **465**, 696 (2010).  
 [13] J. U. Nöckel and A. D. Stone, *Nature* **385**, 45 (1997).  
 [14] C. Gmachl *et al.*, *Science* **280**, 1556 (1998).  
 [15] T. Harayama, P. Davis, and K. S. Ikeda, *Phys. Rev. Lett.* **90**, 063901 (2003).  
 [16] S.-Y. Lee, S. Rim, J.-W. Ryu, T.-Y. Kwon, M. Choi, and C.-M. Kim, *Phys. Rev. Lett.* **93**, 164102 (2004).  
 [17] H. G. L. Schwefel *et al.*, *J. Opt. Soc. Am. B* **21**, 923 (2004).  
 [18] J. Wiersig and M. Hentschel, *Phys. Rev. Lett.* **100**, 033901 (2008).  
 [19] S. Shinohara, T. Harayama, T. Fukushima, M. Hentschel, T. Sasaki, and E. E. Narimanov, *Phys. Rev. Lett.* **104**, 163902 (2010).  
 [20] H. G. L. Schwefel *et al.*, in *Optical Microcavities*, edited by K. Vahala (World Scientific, Singapore, 2004).  
 [21] T. Harayama and S. Shinohara, *Laser Photon. Rev.* **5**, 247 (2011).  
 [22] H. Cao and J. Wiersig, *Rev. Mod. Phys.* **87**, 61 (2015).  
 [23] L. Ge, R. Sarma, and H. Cao, *Optica* **2**, 323 (2015).  
 [24] B. Redding *et al.*, *Proc. Natl. Acad. Sci. USA* **112**, 1304 (2015).  
 [25] T. Fukushima and T. Harayama, *IEEE Select. Topics Quantum Electron.* **10**, 1039 (2004).  
 [26] M. Lebental, J. S. Lauret, R. Hierle, and J. Zyss, *Appl. Phys. Lett.* **88**, 031108 (2006).  
 [27] A. Mekis, J. U. Nöckel, G. Chen, A. D. Stone, and R. K. Chang, *Phys. Rev. Lett.* **75**, 2682 (1995).  
 [28] S.-B. Lee, J.-H. Lee, J.-S. Chang, H.-J. Moon, S. W. Kim, and K. An, *Phys. Rev. Lett.* **88**, 033903 (2002).  
 [29] J. U. Nöckel and A. D. Stone, in *Optical Processes in Microcavities*, edited by R. K. Chang and A. J. Campillo (World Scientific, Singapore, 1996).  
 [30] J. Wiersig, *J. Opt. A, Pure Appl. Opt.* **5**, 53 (2003).  
 [31] S. Shinohara, T. Harayama, H. E. Türeci, and A. D. Stone, *Phys. Rev. A* **74**, 033820 (2006).  
 [32] S.-B. Lee, J. Yang, S. Moon, J.-H. Lee, K. An, J.-B. Shim, H.-W. Lee, and S. W. Kim, *Phys. Rev. A* **75**, 011802(R) (2007).  
 [33] J.-B. Shim *et al.*, *J. Phys. Soc. Jpn.* **76**, 114005 (2007).  
 [34] S. Shinohara and T. Harayama, *Phys. Rev. E* **75**, 036216 (2007).  
 [35] J.-W. Ryu, S.-Y. Lee, C.-M. Kim, and Y.-J. Park, *Phys. Rev. E* **73**, 036207 (2006).  
 [36] S. Shinohara, T. Fukushima, and T. Harayama, *Phys. Rev. A* **77**, 033807 (2008).  
 [37] S. Shinohara, M. Hentschel, J. Wiersig, T. Sasaki, and T. Harayama, *Phys. Rev. A* **80**, 031801(R) (2009).

- [38] S. Shinohara and T Harayama, in *Trends in Nano- and Micro-Cavities*, edited by O'D. Kwon, B. Lee, and K. An (Bentham Science, United Arab Emirates, 2011).
- [39] J. Wiersig and J. Main, *Phys. Rev. E* **77**, 036205 (2008).
- [40] S. C. Creagh, H. B. Hamdin, and G. Tanner, *J. Phys. A: Math. Theor.* **46**, 435203 (2013).
- [41] E. Hecht, *Optics* (Addison-Wesley, Reading, 1987).
- [42] E. Bogomolny, *Nonlinearity* **5**, 805 (1992).
- [43] M. C. Gutzwiller, *J. Math. Phys.* **12**, 343 (1971).
- [44] A. Voros, *J. Phys. A* **21**, 685 (1988).
- [45] T. Harayama, S. Tasaki, and A. Shudo, *Nonlinearity* **12**, 1113 (1999).
- [46] E. Bogomolny, R. Dubertrand, and C. Schmit, *Phys. Rev. E* **78**, 056202 (2008).
- [47] E. Bogomolny, N. Djellali, R. Dubertrand, I. Gozhyk, M. Lebental, C. Schmit, C. Ulysse, and J. Zyss, *Phys. Rev. E* **83**, 036208 (2011).
- [48] A. G. Fox and T. Li, *Bell Syst. Tech. J* **40**, 453 (1961).
- [49] A. E. Siegman, *Lasers* (University Science Books, Mill Valley, 1986).
- [50] T. Fukushima, *J. Lightwave Technol.* **18**, 2208 (2000).
- [51] T. Fukushima, T. Harayama, and J. Wiersig, *Phys. Rev. A* **73**, 023816 (2006).
- [52] M. Hentschel, H. Schomerus, and R. Schubert, *Europhys. Lett.* **62**, 636 (2003).
- [53] M. Choi, S. Shinohara, and T. Harayama, *Opt. Express* **16**, 17554 (2008).
- [54] S. Sunada, T. Fukushima, S. Shinohara, T. Harayama, and M. Adachi, *Phys. Rev. A* **88**, 013802 (2013).
- [55] D. L. Shepelyansky, *Phys. Rev. E* **77**, 015202(R) (2008).
- [56] H. Schomerus and J. Tworzydło, *Phys. Rev. Lett.* **93**, 154102 (2004).
- [57] J. P. Keating, M. Novaes, S. D. Prado, and M. Sieber, *Phys. Rev. Lett.* **97**, 150406 (2006).
- [58] S. Nonnenmacher and M. Zworski, *J. Phys. A* **38**, 10683 (2005).
- [59] M. Novaes, *J. Phys. A: Math. Theor.* **46**, 143001 (2013).
- [60] H. Schanz, *Phys. Rev. Lett.* **94**, 134101 (2005).